Cosmological Dependence of the First Order Power Spectrum Response

Xiaoqi Yu*

Department of Physics, Gustavus Adolphus College

800 West College Avenue, St.Peter, Minnesota 56082, USA

Abstract

We measure the cosmological dependence of the first order power spectrum response to a long wavelength isotropic perturbation using the separate universe simulation method. As a first step, we limit ourselves to explore the cosmological dependence on matter density parameters Ω_m. By taking the amplitude of perturbation to be $\delta_L = \pm 0.05$ for all cosmologies, we find that the value first order response depends on Ω_m. On $k = 2.67$ h/Mpc, the response for matter density parameter on Planck's upper 95% confidence interval of $\Omega_m = 0.3213$ falls 5% below the response for mean density parameter with $\Omega_m = 0.3089$, and the response for density parameter on Planck's lower constrain $\Omega_m = 0.2965$ is about 10% higher than that for the mean. These results also indicate the possible dependence of the responses on other cosmological parameters, which can be found using the same method as we employed here. The cosmological dependence of the responses, which has been neglected before, can be a concern when taking the response approach to measure the higher order statistics of the large scale structure.

*xyu@gustavus.edu

I. INTRODUCTION

The ΛCDM model has emerged as the paradigm to explain the evolution and the structure of the Universe. Numerous astronomical observations have tested the model to high accuracy on scales ranging from a few to thousands of Megaparsecs [1]. In this model the Universe is spatially flat, homogeneous and isotropic on large scales. It is composed of radiation, ordinary matter, non-baryonic cold dark matter, and dark energy. The radiation component includes all the relativistic particles like photons which occupy very small percentage of energy density in the current universe. The ordinary matter, we call it baryons, constitutes galaxies and large scale structures that we can directly observe today, occupies about 5% of the energy density. The non-baryonic cold dark matter (CMD), which only interact gravitationally such that we cannot directly observe by electromagnetic wave, makes up about 25% of the energy density. The dark energy, an unknown form of energy which is hypothesized to permeate through space accelerating the expansion of the universe, constitutes 70% of the energy density. Under the ΛCDM paradigm, the galaxies and the large-scale structure that can be observed today are grown gravitationally from tiny, nearly scale-invariant adiabatic Gaussian-distributed fluctuations in the early universe.

Given that only 5% of the energy components of the universe can be directly observe, one may question the precision of cosmological models with the information merely obtained from observation. There are several ways to probe cosmological models and constrain parameters. The statistical information contained in the large scale structure can help us achieve some precision. The ΛCDM paradigm predicts that the baryons lie within the gravitational potential well of Dark Matter halos. Therefore, the galaxy distribution follows the Dark Matter Halo distribution by a bias factor. N-body simulations, which gravitationally evolve tracers of the matter field, are frequently used to predict the large scale structure in the universe. With simulation, we can model the gravitational behavior of 30% of the energy components of the universe instead of 5% from observation. By experimenting with different models and comparing their statistical properties with those from observation, models and parameters can be constrained. A frequently used method to sample the statistical information in the large scale structure involves n-point correlation functions of the matter density fluctuation field, defined by $\delta(\vec{x}) = \frac{\rho(\vec{x})}{\bar{\rho}} - 1$ at each point $\vec{x}$ in the field, where $\bar{\rho}$ is the mean density for the field[2]. The most well-studied of such is the 2-point correlation function $\xi(r)$ and its Fourier form , the Power Spectrum $P(k = \frac{2\pi}{r})$, which measures the correlation of the density contrast in regions of universe that are separated by distance r. In the linear regime of

structure formation, the Gaussian distributed density field can be entirely described by the power spectrum. Due to non-linearity in the late universe, the growth of structure on different scales is no longer scale-independent. The cosmological information encoded in the large scale structured cannot be completely specified by the power spectrum. Furthermore, different combinations of cosmological parameters might produce power spectrum of similar shape. Therefore higher order statistics are needed to constrain the cosmological parameters to higher precision. However, the complexity of modeling n-point functions increases rapidly with the order n, both analytically through perturbation theory methods and computationally through N-body simulation; it is hence useful to combine perturbation methods and simulation to tackle higher order statistics.

One approach to capture the long- and short- scale coupling in nonlinear gravitational evolution is found in the *Power Spectrum Responses* [3]. These responses measure the fractional changes of the local power spectrum in the presence of long wavelength density perturbation. We can consider them as singling out the higher-order long-wavelength terms of the N-point correlation functions with the long-wavelength modes of density perturbation. The responses can be measured using the *Separate Universe Simulation* methods [4] by the fact that the power spectrum in the local patch under density perturbation is equivalent to the power spectrum of a separated universe with modified cosmological parameters and scaling factor. Ignoring the cosmological dependence of responses, previous authors have used the responses to approximate the squeezed limit of N-point correlation functions[3], and to approach the Power Spectrum Covariance Matrix [5]. However, these higher order statistics studied by previous authors are known to be dependent on cosmology. Therefore, the cosmological dependence of the responses, which has never been studied before, may not be simply negligible. Knowing the dependence of response on cosmological parameters can help us constrain the statistical error in large scale structure measurement using the response approach.

In this work, we summarize the basics of N-Body simulation for matter in Section II. We then introduce the Power Spectrum Responses and their application from the basics of statistical field theory in Section III. The method of measuring the response is summarized in Section IV. Sections V and VI present the results we find and conclusions that can be drawn for the cosmological dependence of the First Order Response. All figures in this work are made by the author.

II. THE BASICS OF N-BODY SIMULATION

Cosmological simulation is an important tool in cosmology. With simulations, we can predict the non-linear regime of large scale structure for various models and cosmological parameters. In the theory of structure formation, each galaxy resides in a host Dark Matter Halo. On large scales, the galaxy distribution hence follows the Dark Matter (referred as DM hereafter) Halo distribution by a bias factor. The baryons, which constitute the galaxies, make up only a small percentage of gravitationally-coupled matter field. The effects of hydrodynamical baryonic processes on small scales can be included in the N-body simulation but are ignored for our purpose of study; baryons and DM are collectively treated as a single collisionless fluid in the simulation. All statistics of the large scale structure are calculated from simulations in this study. We therefore summarize some basics of N-body simulation here.

The N-body simulations normally use discrete tracer particles to approximate the distribution in continuous density field. The dynamics of a tracer particle at location $\vec{x}_i$ is meant to represent the dynamics of the continuous matter around $\vec{x}_i$. These DM tracer particles in simulations can be described by the collionless Boltzmann equation coupled to the Poisson equation in an expanding universe [6]. The simulations evolve the tracer particles gravitationally in a box with continuous boundary condition applied. The gravitational evolution of the particles are characterized by the two equations [7]. The first one is Poisson equation

$$\nabla^2\Phi(\vec{x}) = 4\pi G a^2 \delta\rho(\vec{x}), \tag{1}$$

where a is the scale factor due to expansion such that $a = \frac{1}{1+z}$. Larger redshift z means earlier in time, and z=0 represent the present-day universe. The Poisson equation determines the gravitational potential at each point in the box $\Phi(\vec{x})$, given the density fluctuations $\delta\rho(\vec{x})$. The second one is the force equation

$$\ddot{\vec{x}} + 2H\dot{\vec{x}} = -\nabla\Phi(\vec{x}), \tag{2}$$

which tells the particles how to move. The dots on the top of $\boldsymbol{x}$ represent the time derivative of the tracer particle positions. At each time step in the simulation, the code computes the density field from the particle positions, uses the density field in the Poisson equation to solve for the potential, and plugs the potential into the force equation to move the particles. This process is repeated from some initial redshift z_i , until current day $z = 0$.

III. THE POWER SPECTRUM RESPONSES

A. The Random Field and Power Spectrum

The distribution of any random scalar field $\rho(\vec{x})$ can be described by its overdensity $\delta(\vec{x})$ at each point $\vec{x}$ in the field. The overdensity for all points in the field has

$$\int P(\delta_1, \delta_2, \cdots, \delta_n) d\delta_1 d\delta_2 \cdots d\delta_n = 1, \tag{3}$$

where $\delta_1 = \delta(\vec{x_1})$, and $P(\delta_1, \delta_2, \cdots, \delta_n)$ is the probability of one certain distribution of overdensity in the field. The probability distribution of the overdensity field is specified by its Nth-order moments:

$$\langle \delta_1 \delta_2 \cdots \delta_N \rangle = \int \delta_1 \delta_2 \cdots \delta_N P(\delta_1, \delta_2, \cdots, \delta_N) d\delta_1 d\delta_2 \cdots d\delta_N, \tag{4}$$

where the $\langle\rangle$ denotes the ensemble average of infinite many possible distributions of the field. However, there is one universe available to observe, which forbid us from obtaining many possible distributions. Under Ergodic Hypothesis, the ensemble average of many universe is equivalent to the spatial average taking over all points in one universe, given that the spatial correlation decay rapidly with increasing separation and many statistically independent volumes exists. Therefore, the first moment, which corresponds to the expectation value, always have $\langle \delta \rangle = \frac{1}{V} \int_V \delta(\vec{x}) d^3\vec{x} = 0$. The second moment, which corresponds to the sample variance, is defined to be the two point correlation function assuming homogeneity and isotropy

$$\xi(r) = \langle \delta(x) \delta(x + r) \rangle. \tag{5}$$

Higher order moments indicate e.g. the skewness of the distribution. Infinite many moments are needed to completely specify a cosmological density field which is non-Gaussian [2].

In the context of large scale structure of the universe, the two point correlation function can be intuitively interpreted in the following way: consider a galaxy at point $\vec{x}$, the value for two point correlation function $\xi(r)$ gives the expected probability of finding another galaxy at around distance r from $\vec{x}$ compared to a random field. It is convenient to describe a random field with their Fourier components, such that $\delta(\vec{k}) = \int \delta(\vec{x}) e^{-i\vec{k}\vec{x}} d^3\vec{x}$. Hence, adopting the Fourier convention,

the power spectrum is taken to be the Fourier transform of the two-point correlation function

$$P(k) = \langle |\delta(\vec{k})|^2 \rangle = \frac{1}{2\pi^2} \int \xi(r) \frac{\sin kr}{kr} r^2 dr. \tag{6}$$

During the linear structure formation regime, the distribution of the matter overdensity is Gaussian. Therefore, the N-point probability functions $P(\delta_1, \delta_2, \cdots, \delta_N)$ can be completely specified by the two-point correlation function. The higher moments are 0 since there is no skewness in Gaussian. The initial power spectrum of the universe after inflation can be written as:

$$P_{\text{primordial}}(k) = A_s (\frac{k}{k_*})^{n_s - 1}, \tag{7}$$

where A_s is the amplitude of the primordial curvature power spectrum, k_* is the pivot scale 0.05 Mpc^{-1}, and n_s is the spectral index. The overdensity continues to grow scale-independently in linear regime of structure formation until the overdensity at some location grows sufficiently large such that at $\delta \sim 1$. In the linear regime, the power spectrum can be found as

$$P(k, t) = P_{\text{primordial}}(k) T^2(k) D^2(t), , \tag{8}$$

where $T(k)$ is the transfer function describing the linear relationship between the inflaton fluctuation and later perturbations, and $D(t)$ is the linear growth rate with respective to time which can be calculated from linear density perturbation theory as [8]:

$$\ddot{D} + 2H\dot{D} - \frac{3}{2} H^2 \Omega_m a^{-3} D = 0. \tag{9}$$

When the structure formation enters the nonlinear regime, the overdensity correlations on small scales grow higher than linear prediction. The growth of structure at different Fourier modes are coupled to each other. That means, the growth of structure on smaller scale k is affected by the growth of structure on neighboring modes k'. Hence, Equation 8 can no longer be used to find the power spectrum; numerical simulations are needed to study the mechanism of structure formation.

The Power Spectrum has been well-measured both in observations and simulations. Figure 1 shows the power spectra of the matter density field from one of the simulation we run. The solid black line shows the linearly predicted present-day power spectrum, and the dashed lines show the time evolution of the power spectra, where larger redshift z means earlier in time, and z=0 is the

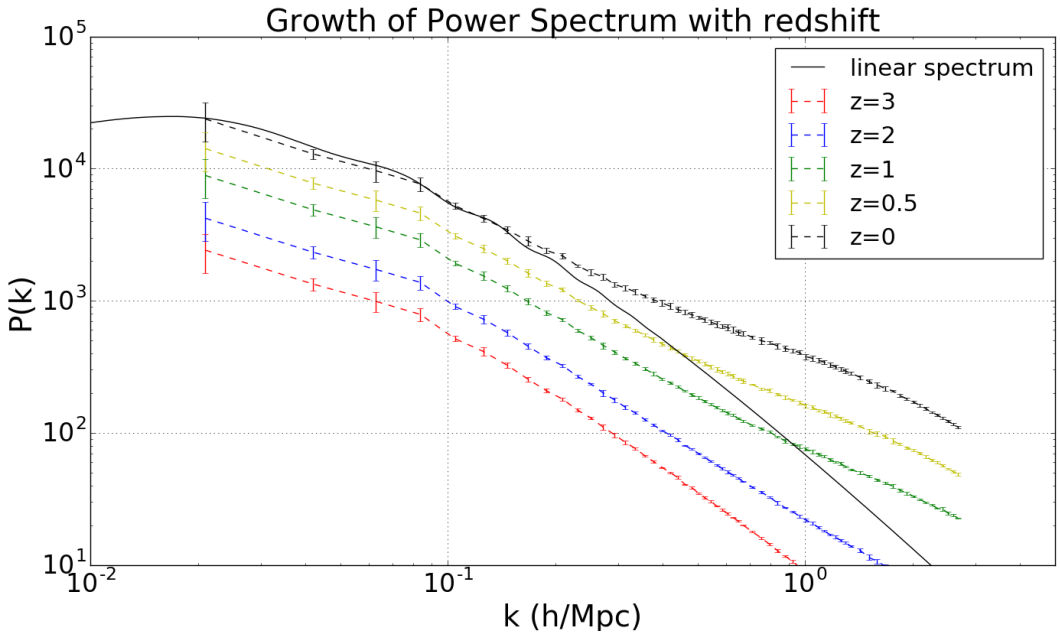

Figure 1: The power spectrum of matter density field from simulation at different redshift. As the universe evolve into present day, the magnitude of power spectrum in the non-linear tail (large k) grow faster than the linear regime (small k)

present-day. The black dashed line by the simulation deviates from the linear prediction at about $k = 0.1$ h/Mpc, meaning that the effect of nonlinear formation appears on scale $r = 2\pi/0.1 \simeq 60h^-1$Mpc for current universe. The time evolution of dashed lines also indicate that the nonlinear structure formation affect small scales first, and larger scale enters nonlinear structure formation regime later.

Another factor that affects the power spectrum is the density of matter component in the universe Ω_m. As shown in the differential equation 9, the matter density parameter shows up in the source term, indicating that the growth rate in the linear regime is higher for high matter density. This is confirmed by Figure 2, which shows the linear and nonlinear power spectrum for different density parameters. At nonlinear regime, the power spectrum deviates from linear prediction roughly at the same scales for all density parameters. Therefore, the power spectrum demonstrates a cosmological dependence in all regime. One may also extrapolate the similar dependence of nonlinear structure formation on matter density in higher order statistics, which we will explore in this work with the cosmological response functions.

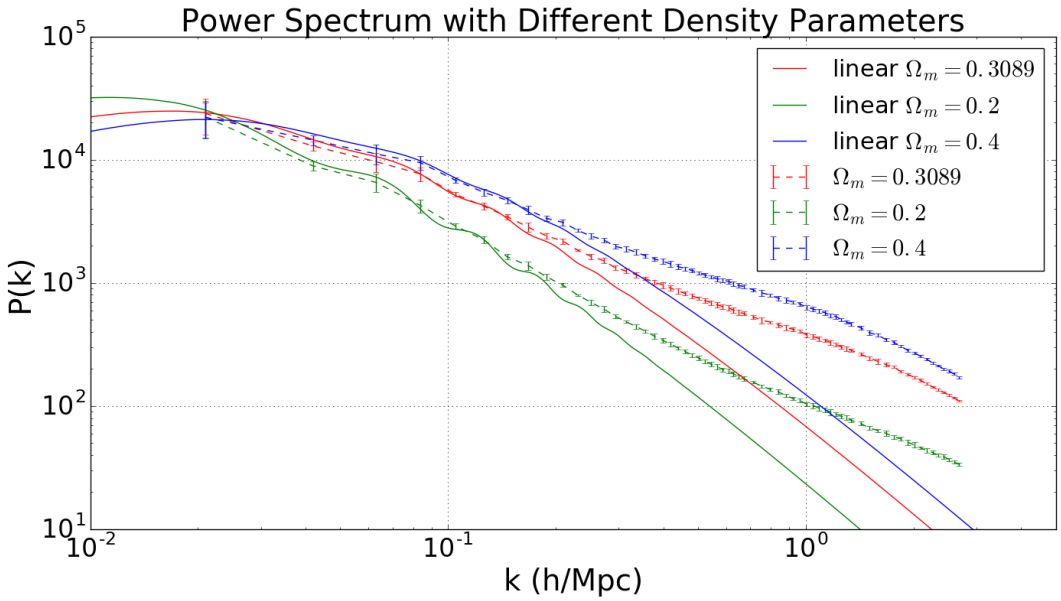

Figure 2: The power spectra of matter density field for current redshift from a set of simulation we run with different matter density parameter.

B. The Response Functions and the Separate Universe Picture

The power spectra of the matter density at low redshifts told us that, as the evolution of the universe enter the non-linear regime, the growth of structure on different modes are no longer independent of each other. It is therefore necessary to use higher order statistics to study the growth of structure in nonlinear regime. However, this is challenging: the number of possible modes increases rapidly with the order of statistics, and the cosmic variance noise within each mode grows significantly. The above reasons make it computationally expensive to sample higher order statistics. A way to reduce the complexity is to study the power spectrum responses, which measure the fractional change of the local power spectrum in presence of long-wavelength perturbations. Figure 3 shows the diagram for small amplitude long-wavelength matter density fluctuation in universe: the overall power spectrum of the background is unchanged by the fluctuation within the universe. However, the power spectra measured in local patches of underdense or overdense regions are modified by the density fluctuation. Within the local patches, the amplitude of perturbation is assumed to be constant. The response functions $R_n(k)$ are defined as the coefficients of the expansion of the power spectrum in linearly extrapolated initial overdensity δ_L [3]:

$$P(k,t|\delta_L) = \sum_{n=0}^{\infty} \frac{1}{n!} R_n(k,t)[\delta_L \hat{D}(t)]^n P(k,t), \tag{10}$$

where $P(k,t|\delta_L)$ is the nonlinear matter spectrum at time t in the presence of an uniform density perturbation with amplitude δ_L in the local patch for current time, $P(k,t)$ is the overall power spectrum in the background universe, and $\hat{D}(t) = \frac{D(t)}{D(t_0)}$ is the modification from linear growth rate that can be calculated from equation 9.

These responses can be broken down into three contributions by considering the patch under perturbation to evolve separately from the background universe. The reference density contribution, which accounts for the difference between power spectra defined with respect to the perturbed local patch and with respect to the background universe, corresponds to $P(k,t)^{\text{ref den}} \equiv [1+\delta_\rho]^2 P(k,t|\delta_L)$, where δ_ρ is the density contrast of the perturbed patch to the background. Another contribution is the dilation effect, which accounts for the perturbation in the local scale factor $\tilde{a}$ due to long wavelength density perturbation, such that $P(k)^{\text{dilation}} \equiv [1+\delta_a]^3 P([1+\delta_a]k,t|\delta_L)$, which $\delta_a = \frac{\tilde{a}}{a} - 1$. The third contribution to the responses comes from the physical changes in the structure induced by the long-wavelength perturbation, which corresponds to actual physical coupling between long- and short-wavelength modes. The first two contributions can be calculated analytically for all scales on any order, and the physical response in the nonlinear regime can be only quantified numerically through simulation. In this work, we focus on the first order response R_1. Summing up the three contributions for the first order, R_1 would have [3]:

$$R_1(k,t) = 1 - \frac{1}{3}\frac{kP'(k,t)}{P(k,t)} + G_1(k,t), \tag{11}$$

where the first term comes from reference density, the second term comes from the dilation effect, with prime denoting derivatives with respect to k, and the third term G_1 is the physical response, named as the *growth-only response*.

One way to measure the physical response G_n in N-body simulations is using the *separate universe* method[4]. The power spectrum of the local patch under a uniform adiabatic density perturbation is equivalent to the power spectrum in a "separate universe", in which the long-wavelength perturbation is absorbed in a modified matter density background in the local patch by modifying the cosmological parameters and curvature. G_1 can be then calculated through simulations by

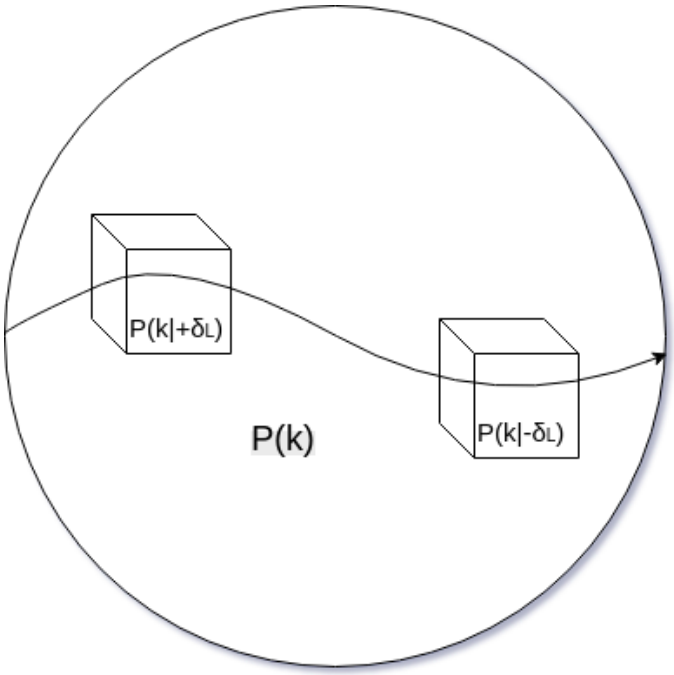

Figure 3: Diagram for universe with long-wavelength matter density perturbation. The background universe is represented by the big circle and the patches of universe under perturbation are shown in boxes. The power spectrum of the background universe is unchanged by the existence of the long-wavelength density fluctuation within the universe. However, the power spectrum of the local patched are modified by the perturbation.

$$\begin{aligned} G_1(k,t) &= \frac{1}{P(k,t)}\left[\frac{d\tilde{P}(k,t|\delta_L)}{d[\delta_L(t)\tilde{D}(t)]}\right]_{\delta_L=0} \\ &\simeq \left[\frac{\tilde{P}(k,t|\delta_L)}{P(k,t)} - 1\right]\frac{1}{\delta_L(t)\tilde{D}(t)}, \end{aligned} \tag{12}$$

where $\tilde{P}(k,t|\delta_L)$ is the power spectrum measured in the separate universe simulation, and $P(k,t)$ is the power spectrum of the background universe.

In the linear regime of structure formation, the growth-only response can be also calculated analytically by replacing power spectra in equation 12 with the square of the linear growth rate $D^2(t)$. The linear first order growth-only response is found to be $G_1^{\text{linear}} = \frac{26}{21}$ [3]. This will be used later to find the sensitivity of the first order response to the nonlinear structure formation.

C. Applications

The responses are useful in various measurements of the large scale structure. For the first order response, the most straight-forward application can be found in measuring the so called angle-averaged squeezed limit of Bispectrum . The Bispectrum is defined as the Fourier transform of the three-point correlation function, $B(\vec{k},\vec{k'},\vec{q}) = \langle\delta(\vec{k})\delta(\vec{k'})\delta(\vec{q})\rangle$ for $\vec{k}+\vec{k'}+\vec{q}=0$. The squeezed limit refer to the cases in which wavenumbers $\vec{k},\vec{k'}$ are larger and $\vec{q}$ is approaching 0 in amplitude. Therefore, $\vec{q}$ corresponds to the wavelength of the uniform density perturbation. The angle-averaged squeezed limit Bispectrum taken over all directions in space is given by[9]:

$$B(k,k',q) = 3!R_1(k)P(k)P_L(q), \tag{13}$$

where $R_1(k)$ is the response, $P(k)$ is the value of short-wavelength mode power spectrum, and $P_L(q)$ is value of the corresponding long wavelength power spectrum.

The Bispectrum has many useful applications. For example, it can be used to constrain inflationary models which predict a non-Gaussian component in the distribution of primordial perturbations that could not be fully illustrated by the power spectrum [10]. By taking the response approach for the Bispectrum, the computational complexity is largely reduced.

Another application of the first order response is found in evaluations of the power spectrum covariance matrix, defined as[11]:

$$\begin{aligned}\mathrm{Cov}(\vec{k_1},\vec{k_2}) &= \langle\hat{P}(\vec{k_1})\hat{P}(\vec{k_2})\rangle - \langle\hat{P}(\vec{k_1})\rangle\langle\hat{P}(\vec{k_2})\rangle \\ &= \mathrm{Cov}^{\mathrm{G}}(\vec{k_1},\vec{k_2}) + \mathrm{Cov}^{\mathrm{cNG}}(\vec{k_1},\vec{k_2}) + \mathrm{Cov}^{\mathrm{SS}}(\vec{k_1},\vec{k_2}).\end{aligned} \tag{14}$$

The covariance matrix could be used to quantify the statistical error in measurements of the power spectrum from upcoming large scale structure surveys. The estimation of the covariance by simulation only can be cumbersome since many realizations are needed to sample the ensemble average. An alternatively way is to combine perturbation method and simulations. By doing this, the calculation of the covariance can be broken down into three contributions as shown above in Eq.14: the Gaussian (G) covariance, which is the diagonal term that can be calculated directly from power spectrum; the connected non-Gaussian (cNG) term which is induced by mode-coupling in nonlinear structure formation [5]; and the super sample covariance (SS) which accounts for the correlation between the modes that can be observed and modes whose wavelength is larger than

the survey size. This may happen when the observed region in survey is embedded in a large-scale super-survey overdensity, which is the same as the case which defines the power spectrum responses for a patch of universe is embedded in a region under long wavelength perturbation. Therefore, the super sample covariance can be completely captured by the first-order responses. For the angle-averaged spectra and isotropic survey window, the covariance can be obtained by [9]:

$$\begin{aligned} \mathrm{Cov}^{\mathrm{SS}}(k_1, k_2) = &\left[\frac{1}{V^2}\int \frac{d^3\vec{q}}{(2\pi)^3}|\tilde{W}(\vec{q})|^2 P_{\mathrm{L}}(q)\right] \\ &\times R_1(k_1)P(k_1)R_1(k_2)P(k_2), \end{aligned} \tag{15}$$

where $\tilde{W}(\vec{q})$ is the Fourier transform of the survey window function, V is the volume of the survey, and the $P(k)$s are the theoretical predictions for the values of power spectrum at k_1 and k_2 respectively.

Given that the growth of structure on different scales depends on cosmological parameters, Bispectrum and Covariance matrix are also cosmological dependent. In taking the response approach for these measurement, it is therefore necessary to take the possible cosmological dependence of R_1 into consideration. However, previous authors have been assuming the cosmological dependence of R_1 to be negligible. The goal of this work is to investigate if cosmological dependence of responses is a concern to evaluate higher order statistics.

IV. METHODOLOGY

In order to quantify the dependence of first order response function on different matter density parameters, cosmologies with different Ω_m are matched by the same primordial density power spectrum $P_{\text{primordial}}(k) = A_s(\frac{k}{k_*})^{n_s-1}$. This is accomplished by the Boltzmann-Einstein code **CAMB**[12] in which we specify the parameters A_s and n_s. The **CAMB** code calculates the linear matter power spectrum for current time according to equation 8 by specifying also the following cosmological parameters: $\Omega_b h^2$, $\Omega_c h^2$, $\Omega_\nu h^2$, and Ω_k, which are respectively the density parameter for baryon, Cold Dark Matter, cosmic neutrino, and curvature. h is the Hubble rate such that $H = 100h\frac{\text{km/s}}{\text{Mpc}}$. The matter density parameter can be obtained by $\Omega_m = (\Omega_b h^2 + \Omega_c h^2 + \Omega_\nu h^2)/h^2$. In this work, we approximate the cosmic neutrinos to be massless $\Omega_\nu = 0$.

For each set of Ω_m, the initial conditions of the simulations (ie, the initial position and velocity distribution of simulation tracer particles) are created both in fiducial cosmology and in the separate universes. This is done by the **ic_curved** code [4] which reads the linear power spectrum at current redshift from **CAMB**'s calculation, and rescale it to the initial condition $z_i = 49$ for each cosmology with $[\tilde{D}(\tilde{a}_i)\tilde{D}(\tilde{a}=1)/D(a=1)]^2$. The **ic_curved** code also calculates the rescaled box size $\tilde{L}$ and the cosmological parameters $[\tilde{\Omega}, \tilde{h}]$ in the separate universe for given amplitude of long-wavelength perturbation δ_{L0}, particle number Np, box size L, and corresponding fiducial parameters $[\Omega, h]$. It then generates a Gaussian realization of the density field that matches the linear matter power spectrum at $z = 49$ and the rescaled parameters for each cosmology.

The **Gadget-2** code [6] is used to carry out the N-body simulation. For each simulation, **Gadget-2** reads the initial positions and velocities of particles from the Gaussian realization generated by ic_curved, and evolves the particles gravitationally from initial condition to current time in the cubic box with size specified by the initial condition. **Gadget-2** writes snapshots for the particle positions and velocities at redshifts specified by the user. The matter power spectrum for each snapshot is measured by the **Powmes** [13] code.

In this work, we adopt a flat ΛCMD cosmology with $\Omega_m = 0.3089$, $h = 0.6774$, $n_s = 0.9667$, and $A_s = 2.142 \times 10^{-9}$ from **PLANCK** observation [14] for the reference fiducial cosmology. Ω_m= 0.2 and Ω_m= 0.4 are chosen to investigate the cosmological dependence. For all Ω_m values, uniform density perturbation with $\delta_L = \pm 0.05$ is taken for the separate universe simulations. For each cosmology, 5 realizations of the Gaussian random field with 256^3 particles are run in 300 h^{-1}Mpc box. For one set of simulations, we keep the random seed for realization to be the same, and increase the mass resolution to 512^3 particles and box size to 800 h^{-1}Mpc respectively for use as a convergence test.

V. RESULT

A. The Convergence tests

We ran one realization of the simulation with 512^3 particles in 800 h^{-1}Mpc box to check its convergence with linear prediction for G_1 on large scales. It is predicted that, on some sufficiently large scale, the simulation should agree with linear prediction $G_1^{\text{linear}} = \frac{26}{21}$. However, in smaller boxes, the simulation might not be able to sample the response on such scale due to sampling

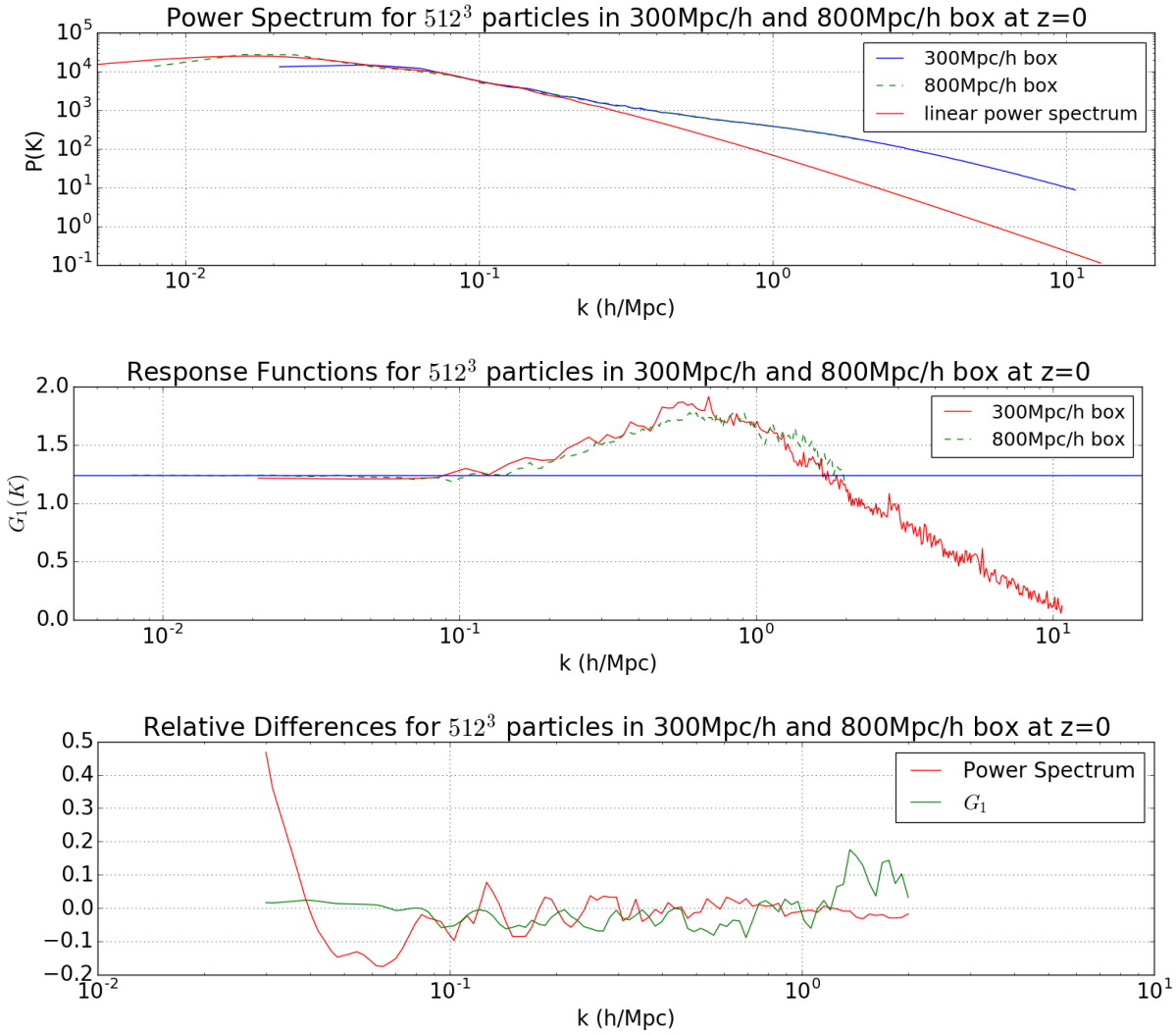

Figure 4: Convergence Test for Box sizes. Top: The power spectrum of matter density field at redshift z=0 with 512^3 particles in 300 h^{-1}Mpc and 800 h^{-1}Mpc box. Middle: first order growth only response function G_1 at redshift z=0 with 512^3 particles in 300 h^{-1}Mpc and 800 h^{-1}Mpc box. Bottom: The relative difference in power spectrum and in response of 800 h^{-1}Mpc box simulation from 300 h^{-1}Mpc box simulation.

variance and lack of modes on large scales. As shown in the middle panel of Figure 4, the 800 h^{-1}Mpc box simulation agrees with the linear prediction up to $k = 0.05$ h/Mpc, where nonlinearity start to have a effect on G_1. Therefore, our simulations with Gadget can be trusted for validity. The 300 h^{-1}Mpc box simulation with one realization are not able to sample with precision at such large scale due to lack of modes, which explains the divergence from linear prediction. For the same random seed at initial condition, the first order response has better convergence than the power spectrum on large scale for different box size as shown in the lower panel of Figure 4. With averaging 5 realization in 300 h^{-1}Mpc box, the measured G_1 also agree with linear

prediction on scale up to $k = 0.05$ h/Mpc at redshift $z = 0$, as shown in lower left panel of Figure 6. Therefore, the 300 h^{-1}Mpc box simulation can be trusted down to its fundamental mode for measuring responses.

Convergence test against particle number is carried out to determine the smallest scale in k-space that can be trusted for the 256^3 particles in 300 h^{-1}Mpc box simulations. As shown in figure 5, the power spectrum in 300 h^{-1}Mpc box for 256^3 particles diverges from that for 512^3 particles for $z \geq 2$, the reasons for this discrepancy are unknown. Here, we skip a thorough investigation of this and focus on simulation output at redshifts z=1, 0.5 and 0, where the two mass resolutions agree well. At small scale, simulations with 256^3 and 512^3 particles agrees with each other for both power spectrum and first order response functions. The Nyquist frequency for 256^3 particles in 300 h^{-1}Mpc is found at $k = 2.67$ h/Mpc. Hence, our simulations can be trusted at the range of $k = [0.02, 2.67]$ h/Mpc for redshift z= 1, 0.5 and 0.

B. Dependence on Ω_m of the First Order Growth Only Responses

The left panels of Figure 6 show the first order growth only response G_1 for different cosmologies at redshifts z=1, 0.5, and 0 as labeled. The G_1 measured from 5 realizations of simulations for fiducial cosmology with $\Omega_m = 0.3089$ is shown in blue curves. The response in fiducial cosmology always has a maximum value at each redshift, the value of the maximum response does not change significantly with time but the scale that the maximum corresponds to moves toward larger scale as the structure formation approaches current time. This tells us that the scale that is most impacted by a long wavelength perturbation grows larger as the universe evolves.

The shape of the response is dependent on the cosmological parameter, as shown in the red curves for $\Omega_m = 0.4$ and green curves for $\Omega_m = 0.2$: The values of response decrease with increasing matter density parameter on all scales for all redshifts. The scale that the maximum response corresponds to grow larger with time for all cosmologies. At each redshift, the scale that the long wavelength perturbation impact the most is larger for higher density parameter. The percentage differences of G_1 for modified density parameter cosmologies and G_1 for fiducial cosmology are shown on the right panel. The percentage differences, however, does not change significantly with different redshifts. The variance in the relative difference predicted by the 5 realizations of simulations grows larger as the structure formation approaches current day. This can be understand by the fact that as time goes by, the increasing nonlinearity on small scales

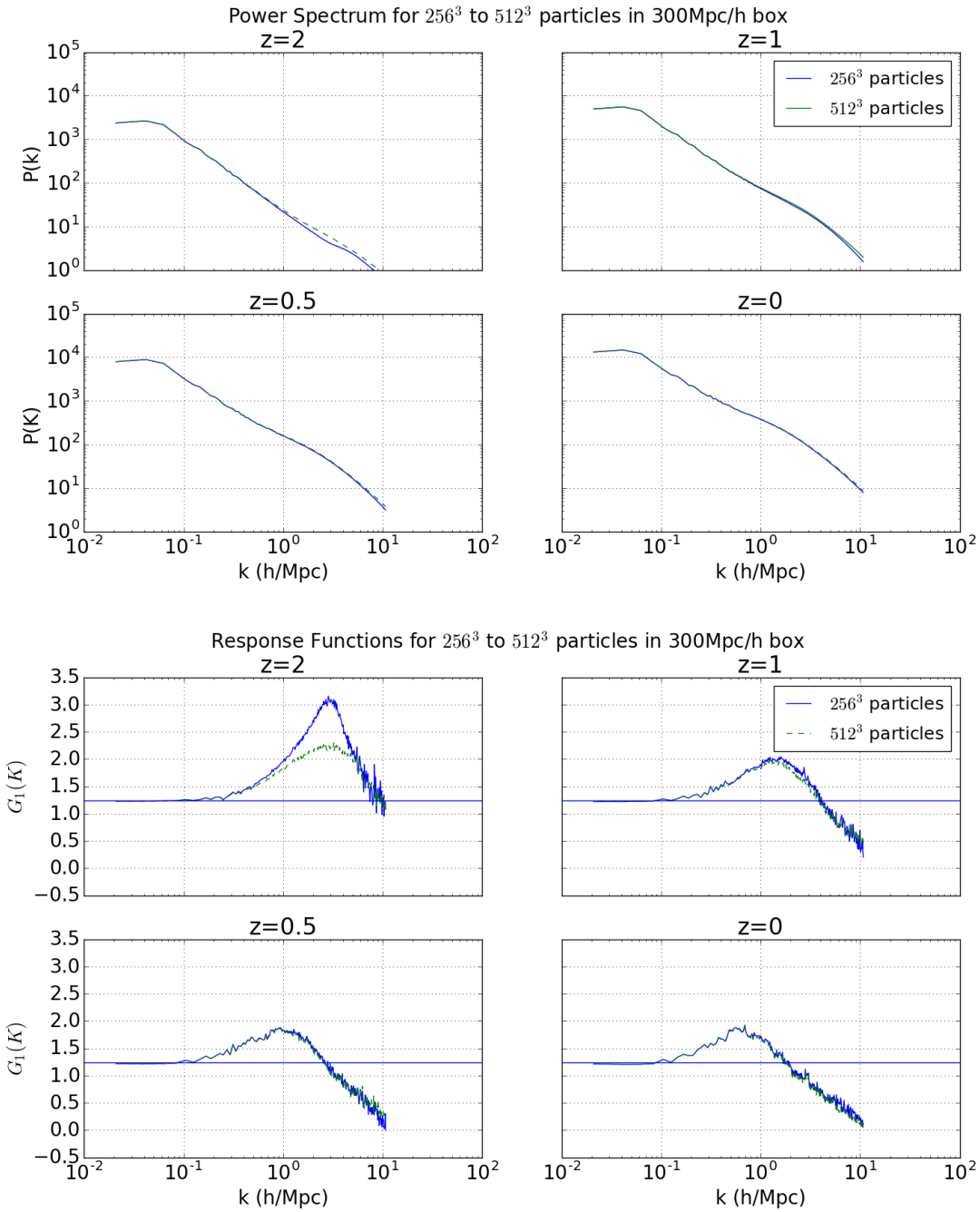

Figure 5: Convergence Test for Particle Numbers. Top: The power spectrum of matter density field at redshift z= 2, 1, 0.5, and 0 with 256^3 and 512^3 particles in 300 h^{-1}Mpc box. Bottom: first order response function at redshift z= 2, 1, 0.5, and 0 with 256^3 and 512^3 particles in 300 h^{-1}Mpc box.

works to "erase memory" from the initial conditions, which effectively increases the variance in the N-body simulations for the response measurement. We also notice that the relative difference is not symmetric from 0 although the density parameters Ω_m on 0.2 and 0.4 is almost symmetric from $\Omega_m = 0.3089$. This might be caused by the fact that we use the same absolute magnitude of

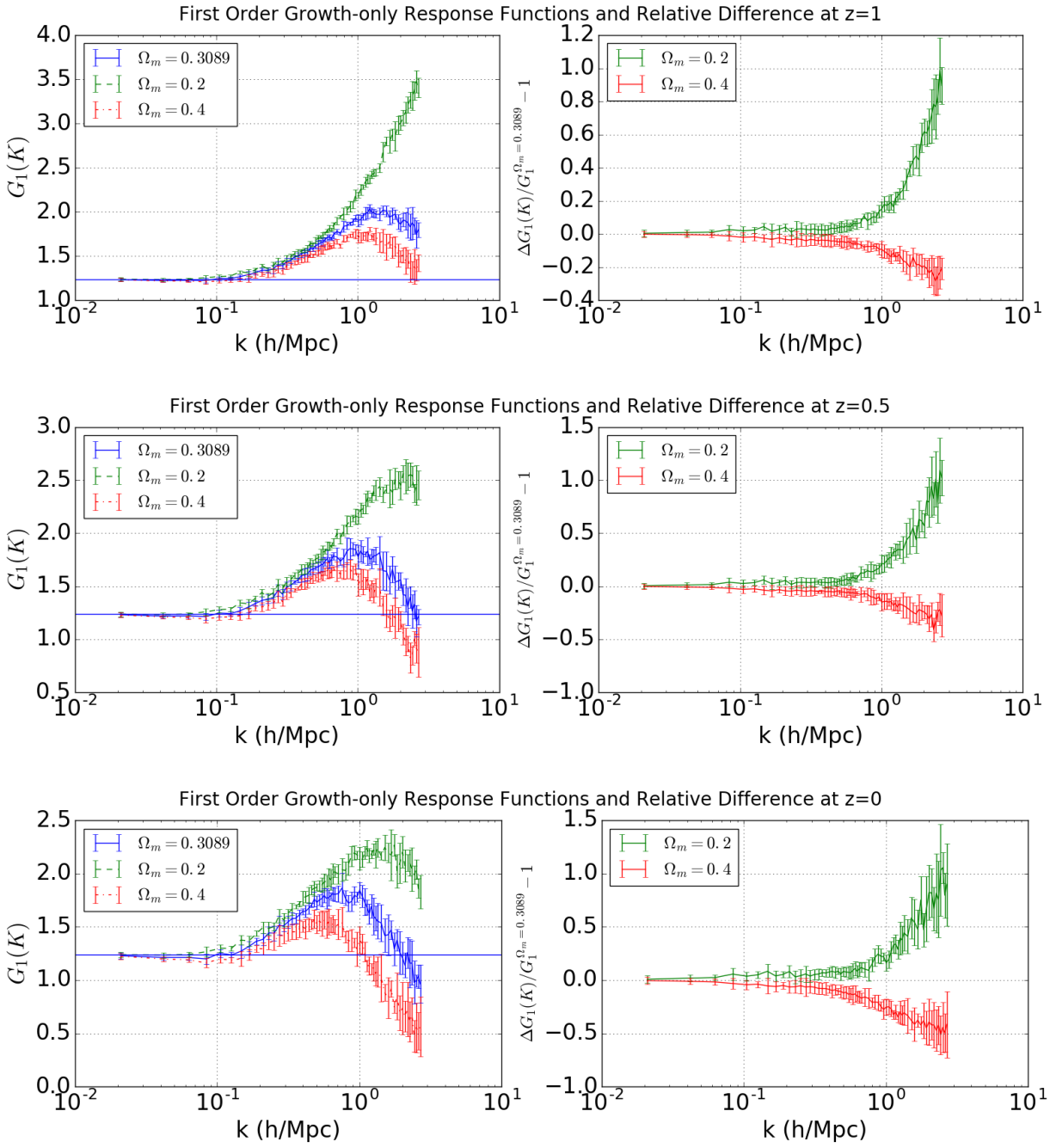

Figure 6: First Order Growth Only Response G_1 for cosmologies from 5 realizations of the separate universe simulations with different density parameters (fiducial from Planck, others chosen at $\Omega_m = 0.2$ and $\Omega_m = 0.4$), and the relative difference in G_1 of modified from fiducial at redshifts z=1, 0.5 and 0.

perturbation $\delta_L = 0.05$ for all three cosmologies, so the relative magnitude of perturbation would be significantly higher for $\Omega_m = 0.2$ than that for $\Omega_m = 0.4$.

PLANCK reported the density parameter to be $\Omega_m = 0.3089 \pm 0.0062$ from recent observation [14], where the uncertainty represent 1σ. In order to make our response measurements valuable for

observational purposes, we use linear interpolation to predict the first order growth only responses G_1 for matter density parameters within 95% confidence interval of PLANCK's prediction. The result for interpolation at each redshift are shown in Figure 7. The G_1 predicted for mean. upper 95% confidence interval, and lower 95% confidence interval of Ω_m values from PLANCK are shown by the solid black line, short black dashed lines, and long black dashed lines respectively. We also show in the lowest panel of Figure 7 the relative difference of the first order growth only responses for density parameters at Planck's limit from that at Planck's mean for redshift z=0.5: At $k = 2.67$ h/Mpc, the response for PLANCK's upper 2σ limit of density parameter $\Omega_m = 0.3213$ is about 5% lower than the response for mean, and the response for lower 2σ limit $\Omega_m = 0.2965$ is about 10% higher than the mean. Therefore, the response is cosmological dependent within PLANCK's measured range of matter density parameter. However, the difference in theses responses lies within the statistical uncertainty of our response measurement for the mean density parameter. More realizations of simulations are needed to narrow down the uncertainty in the response measurement for each cosmology.

VI. CONCLUSION

In this study, we use N-body simulations and the separate universe method to measure the first order growth only matter power spectrum response for different matter density parameters Ω_m. The response tells us how in the power spectrum of the local universe changes in presence of a long-wavelength overdensity perturbation. In this work, the amplitudes of the long-wavelength perturbation are set to be the same for all density parameters. We measured the responses for $\Omega_m = 0.2, 0.3089,$ and 0.4, and we found that the power spectrum response has cosmological dependence. The values for the response decrease with increasing matter density parameters on all scale for redshifts z=1, 0.5, and 0 as shown in Figure 6.

In order to make our measurement meaningful for observational purposes, we use linear interpolation to predict G_1 for cosmological parameters within 95% confidence interval of PLANCK's measurement $\Omega_m = 0.3089 \pm 0.0062$, where the uncertainty represent 1σ. The response is found to be cosmological dependent within PLANCK's measured range of matter density parameter as shown in Figure 7. At redshift z=0.5, the first order response varies by 3% within planckâĂŹs 2σ bounds on $k = 1$ h/Mpc. On scale of $k = 2.67$ h/Mpc, the response for Planck's upper limit of density parameter $\Omega_m = 0.3213$ falls 5% below the response for mean, and the response for

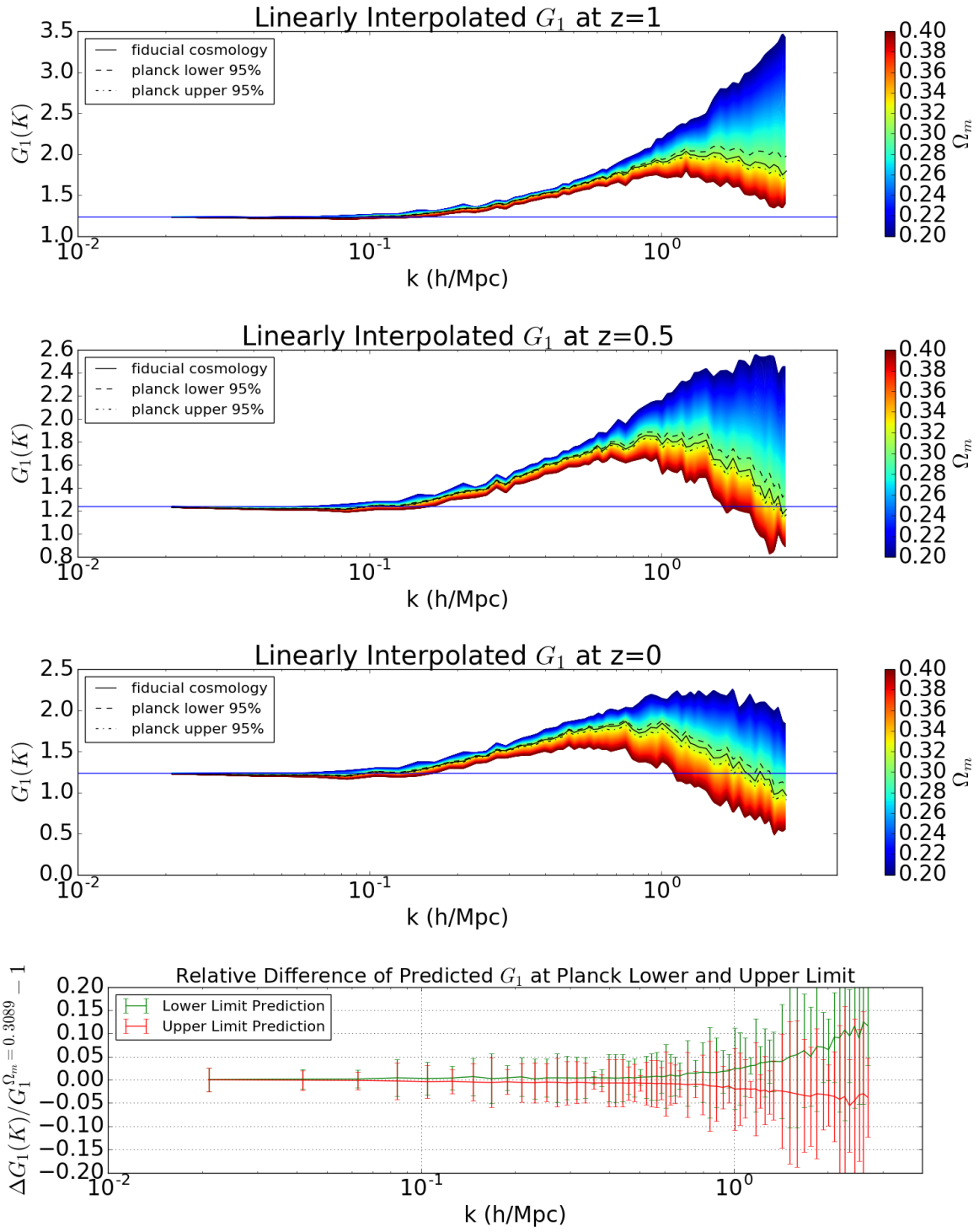

Figure 7: Predicted cosmological dependence of First Order Growth Only Response G_1 at redshifts z=1, 0.5 and 0. The solid black lines show the responses for mean density parameter from PLANCK's measurement. The dashed black lines shows the responses for density parameters within PLANCK's 95% confidence interval $\Omega_m = [0.2965, 0.3213]$. The lowest Panel shows the predicted percentage difference in G_1 for density parameters on Planck's upper and lower limits of confidence interval compared to the mean density parameter at redshift z=0.5 .

lower limit $\Omega_m = 0.2965$ is about 10% higher than the that for mean. However, the difference in these responses lies within the statistical uncertainty of the response measured by our simulations for the mean density parameter. More realizations of simulation are needed to narrow down the uncertainty in response measurements.

Our results show that the cosmological dependence of the responses can be important when taking the response approach to measure the higher order statistics of the large scale structure, which has been ignored in previous studies. More study is needed to robustly determine the dependence of first order response on matter density parameters. The approach we have taken here can be also applied to find the cosmological dependence of the responses on other cosmological parameters (eg h, A_s, and n_s). Precisely finding the cosmological dependence of the responses can help us further calculate the power spectrum covariance matrix and the N-point correlation functions with the high accuracy that is expected to achieve in upcoming large-scale structure surveys.

Acknowledgments

This work is finished as a part of the EuroScholars visit at Ludwig Maximilian Universität Múnchen and Max Planck Institute for Astrophysics under supervision of Dr. Alexandre Barreira. Xiaoqi acknowledges supports from Gustavus Adolphus College, the EuroScholars program, and the Thomas D. Rossing Fund for Physics Education.

---

[1] G. Hinshaw, D. Larson, E. Komatsu, D. N. Spergel, C. L. Bennett, J. Dunkley, M. R. Nolta, M. Halpern, R. S. Hill, N. Odegard, et al., The Astrophysical Journal Supplement **208**, 19 (2013), 1212.5226.

[2] F. Bernardeau, S. Colombi, E. Gaztañaga, and R. Scoccimarro, Physics Reports **367**, 1 (2002).

[3] C. Wagner, F. Schmidt, C.-T. Chiang, and E. Komatsu, Journal of Cosmology and Astroparticle Physics **8**, 042 (2015), 1503.03487.

[4] C. Wagner, F. Schmidt, C.-T. Chiang, and E. Komatsu, Monthly Notices of the Royal Astronomical Society **448**, L11 (2015), 1409.6294.

[5] A. Barreira and F. Schmidt, Journal of Cosmology and Astroparticle Physics **11**, 051 (2017),

1705.01092.

[6] V. Springel, Monthly Notices of the Royal Astronomical Society **364**, 1105 (2005), astro-ph/0505010.

[7] H. A. Winther, F. Schmidt, A. Barreira, C. Arnold, S. Bose, C. Llinares, M. Baldi, B. Falck, W. A. Hellwing, K. Koyama, et al., Monthly Notices of the Royal Astronomical Society **454**, 4208 (2015), 1506.06384.

[8] J. A. Frieman, M. S. Turner, and D. Huterer, Annual Review of Astronomy & Astrophysics **46**, 385 (2008), 0803.0982.

[9] A. Barreira and F. Schmidt, Journal of Cosmology and Astroparticle Physics **2017**, 053 (2017).

[10] A. Lazanu, T. Giannantonio, M. Schmittfull, and E. P. S. Shellard, Physical Review D **93**, 083517 (2016), 1510.04075.

[11] A. Barreira, E. Krause, and F. Schmidt, ArXiv e-prints (2017), 1711.07467.

[12] A. Lewis, A. Challinor, and A. Lasenby, Astrophysical Journal **538**, 473 (2000), astro-ph/9911177.

[13] S. Colombi, A. Jaffe, D. Novikov, and C. Pichon, Monthly Notices of the Royal Astronomical Society **393**, 511 (2009), 0811.0313.

[14] Planck Collaboration, N. Aghanim, Y. Akrami, M. Ashdown, J. Aumont, C. Baccigalupi, M. Ballardini, A. J. Banday, R. B. Barreiro, N. Bartolo, et al., Astronomy & Astrophysics **594**, A13 (2016), 1502.01589.